Journal of The Electrochemical Society, **151** (8) F178-F181 (2004)
0013-4651/2004/151(8)/F178/4/$7.00 © The Electrochemical Society, Inc.

Comparison of Curing Processes for Porous Dielectrics

Measurements from Specular X-Ray Reflectivity

Ronald C. Hedden,[a,c,z] Carlo Waldfried,[b] Hae-Jeong Lee,[a] and Orlando Escorcia[b]

[a]*National Institute of Standards and Technology, Polymers Division, Gaithersburg, Maryland 20899, USA*
[b]*Axcelis Technologies, Incorporated, Rockville, Maryland 20855-2798, USA*

Specular X-ray reflectivity (SXR) was employed to compare structure and barrier properties of a series of nanoporous organosilicate low dielectric constant (low-*k*) thin films cured by several different techniques. The polymethylsilsesquioxane films were prepared by curing the same starting material by five different techniques: standard furnace cure, a novel UV light-assisted process, and three plasma-assisted processes. The films' electron density *vs.* depth profile, pore volume fraction, and moisture uptake were measured by SXR. The measurements illustrate how curing technology can significantly impact low-*k* film structure and barrier properties and also illustrate the value of SXR for characterization of depth-dependent phenomena in nanoporous thin films.
© 2004 The Electrochemical Society. [DOI: 10.1149/1.1766311] All rights reserved.

Manuscript submitted August 4, 2003; revised manuscript received January 22, 2004. Available electronically July 9, 2004.

Curing is an integral process step in the production of many porous low dielectric constant materials (low-*k* dielectrics). Because the traditional vertical furnace cure method requires longer cure times and high temperatures, alternative cure methods such as plasma- or UV-assisted processes are of great interest in the semiconductor chip manufacturing industry. These alternative approaches require significantly reduced curing times and, in many cases, lower cure temperatures.[1-7] Lower cure temperatures are desired to minimize the thermal budget, reducing device failures during curing of back-end-of-line dielectric layers. Over the past year, plasma and UV cure processes have been investigated on polymethylsilsesquioxane (MSQ)-type low-*k* thin films.[2] Plasma processes can increase the mechanical strength of porous low-*k* dielectrics by providing additional cross-linking of the film.[3-7] Although plasma- and UV-cured MSQ films have shown comparable or improved electrical, physical, and chemical properties, evaluation of additional material properties is of great interest. Currently, it is desired to identify alternative processes that produce dielectric films having structural, barrier, and dielectric characteristics closely resembling those of the furnace-cured film, while providing improved mechanical properties and lowered thermal budget.

Previous work has established specular X-ray reflectivity (SXR) as a versatile tool for the characterization of nanoporous film electron density depth profile, thickness, porosity, and solvent or moisture uptake.[8-12] Because of its depth resolution, SXR is an outstanding tool for distinguishing subtle differences in film properties induced by different curing processes. To illustrate how SXR is useful for probing film structure and barrier properties, SXR experiments have been conducted on a representative MSQ material cured by several techniques.

Experimental

All samples were JSR Corporation LKD-5109,[d] an organosilicate spin-on MSQ type dielectric. The first step in the curing sequence of LKD-5109 is spin coating of the precursor material onto a substrate at 2000-3000 rpm, depending on the desired film thickness. This step is followed by a hot plate "prebake" in air at 80°C for 60 s to evaporate solvents and a 60 s hot plate "softbake" at 200°C in air, which initiates cross-linking of the MSQ resin. The final cure is typically done in a vertical furnace at ambient pressure in nitrogen with controlled temperature ramping to 420°C, at which temperature the dielectrics are cured for at least 30 min. The uncured starting material contains partially cross-linked MSQ containing hydrophobic methyl groups and curable silanol (Si-OH) groups that can condense during curing to liberate water and form Si—O—Si linkages. Without any further treatment, the cured films can still contain some unreacted silanols. A subsequent treatment with hexamethyldisilazane (HMDS) may or may not be conducted to convert residual silanols to less polar methyl-terminated species.

In this study, sample 1 is the starting material after prebake and softbake, but without the final cure step (hereafter called "uncured"). Samples 2-5 are the finished products cured by RapidCure processes from Axcelis Technologies, Inc. The plasma cures utilize one of three plasma chemistries (N_2/CH_4, $N_2/H_2/CF_4$, or N_2/H_2) in a downstream plasma curing tool, typically at chamber pressures of 400-500 Pa, and wafer temperatures of up to 420°C. The process time is approximately 2 min. UV curing conditions involve exposure of the dielectric to a broadband UV light source in a He purged environment at atmospheric pressure with reduced oxygen content at wafer temperatures of less than 400°C. The typical UV cure process time is about 2 min. Sample 2 was UV cured; sample 3 was N_2/CH_4 plasma cured; sample 4 was N_2/H_2 plasma cured, then treated with HMDS vapor by an experimental process designed to make the samples hydrophobic; and sample 5 was $N_2/H_2/CF_4$ plasma cured. Sample 6 was subjected to a standard vertical furnace cure at 425°C. All samples were prepared from the same batch of starting material to maintain consistent precursor thickness and properties.

The SXR was measured using a high-resolution reflectometer capable of characterizing films up to 1.5 μm thick.[12] Data were collected in the specular condition (with the grazing incident angle Ω equal to the detector angle θ), and the reflected intensity was recorded as a function of angle. The film thickness, surface roughness, and electron density profile were deduced using a computer modeling routine capable of simulating reflectivity from multilayer structures. To deduce porosity and moisture uptake, additional SXR experiments were conducted inside an environmental control chamber equipped with X-ray transparent Be windows. For toluene uptake experiments, the films were exposed to saturated toluene vapor for 2 h or more prior to measuring SXR data. For water uptake experiments, the films were exposed to saturated water vapor for 3 h prior to measuring SXR data. Unless otherwise stated, uncertainties in all reported quantities are standard deviations based on the goodness of the fits. Total combined uncertainties are not reported, as comparisons are made with data obtained under the same conditions.

Results and Discussion

The first experiments consisted of measuring SXR in air under ambient conditions (Fig. 1). SXR data are plotted as log(reflected intensity/incident intensity) *vs.* q. The scattering vector q is related to the reflected angle θ by $q = (4\pi \sin\theta)/\lambda$, where λ is the X-ray

[c] Present address: Department of Materials Science and Engineering, The Pennsylvania State University, University Park, PA 16802.
[z] E-mail: hedden@matse.psu.edu

[d] Certain commercial materials and equipment are identified in this paper to adequately specify the experimental procedure. In no case does such identification imply recommendation by the National Institute of Standards and Technology, nor does it imply that the material or equipment is the best available for this purpose.

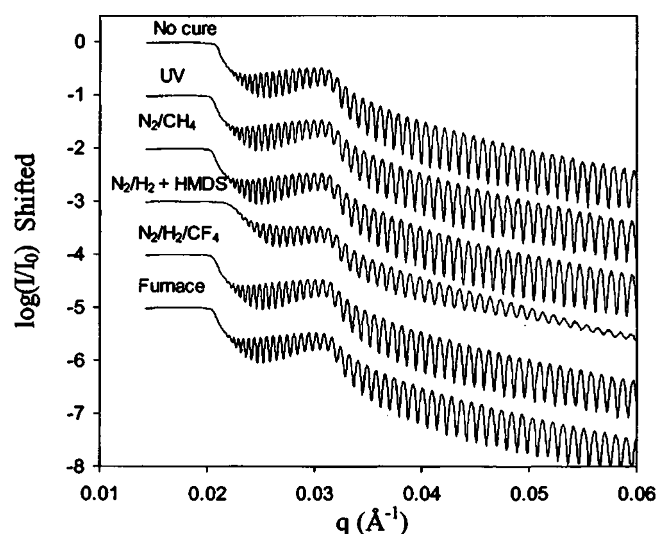

Figure 1. SXR data for all samples in air.

wavelength. The well-defined reflectivity fringes in Fig. 1 indicate that the samples have relatively smooth surfaces. The best fits obtained by computer modeling gave the thickness and density data listed in Table I. The surface roughness was modeled as an interfacial layer at the film-air interface with a density gradient described by an error function. The roughnesses quoted represent the total thickness of this interfacial layer determined from the best fit to the data. From a knowledge of atomic composition, the film electron densities were converted to average mass densities (including porosity) reported in Table I. The reflectivity data for sample 4 (N_2/H_2 plasma cure + HMDS) were best represented by a nonuniform electron density profile (multilayer structure). The data for the other five samples were well described by fits to uniform (single-layer) profiles. Fits are not shown in Fig. 1 for clarity, as the fits were nearly identical to the measured reflectivity data.

The thickness of the films can be deduced from the spacing of the fringes at high q, which are closer together for thicker films. Uncertainties in all reported thicknesses are estimated at ± 20 Å. The measured thickness of the uncured sample was (6180 ± 20) Å. Compared to the uncured sample, all of the cured samples were reduced in thickness by approximately 1-3%, with the exception of sample 4 (N_2/H_2 + HMDS), which was reduced by about 6.5%. The surface roughness of the films was approximately 20 Å for all of the samples. Compared to the uncured sample (1), four of the cured samples (2, 3, 5, and 6) had a slightly lower bulk density. All these samples exhibited only a marginal change in thickness after curing, and none was subsequently treated with HMDS. The very slight decrease in bulk density during curing likely occurred by loss of mass in the form of water vapor due to condensation of the silanols. In contrast, sample 4, which decreased in thickness during curing and was subsequently treated with HMDS, had a slightly higher bulk density than the uncured material. The observed increase in density may be due to a combination of factors: densification from shrinkage (*i.e.*, loss of porosity) and addition of mass in the form of methyl groups by HMDS treatment.

Table I. Summary of SXR results. Uncertainties quoted in text.

Sample	Thickness (Å) air/toluene/water	Porosity	Bulk density (g cm^{-3})	H_2O uptake (mass frac.)
1 No cure	6180/6235/6140	0.38	1.03	0.263
2 UV	6080/6140/6120	0.41	0.99	0.351
3 N_2/CH_4 plasma	6075/6100/6080	0.41	0.99	0.026
4 N_2/H_2 + HMDS	5780/5970/5970	0.35	1.07	0.085
5 $N_2/H_2/CF_4$ plasma	6065/6090/6070	0.40	1.00	0.040
6 Furnace cure	6030/6050/6025	0.40	1.00	0.006

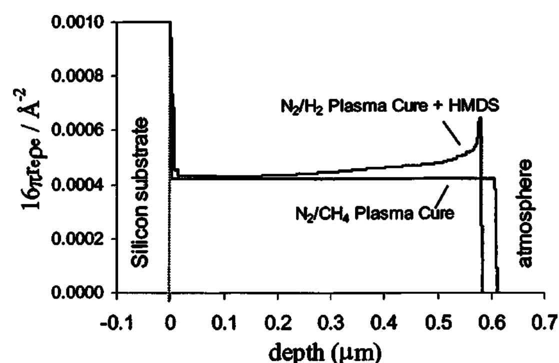

Figure 2. Electron density depth profiles for two plasma-cured films.

Using the computer modeling routine, the film electron density was modeled as a function of depth. Figure 2 shows calculated electron density profiles for two of the plasma-cured samples: N_2/CH_4 plasma and N_2/H_2 plasma + HMDS. Density profiles are plotted as $(16\pi r_e \rho_e)$ *vs.* film depth, where r_e is the radius of an electron, taken to be 2.82×10^{-5} Å, and ρ_e is the electron density ($e^-/Å^3$). The reflectivity data for the N_2/CH_4 plasma-cured film was best modeled by a single layer of uniform electron density. Density depth profiles of the uncured film, the furnace-cured film, and the UV-cured film (not shown) were also uniform, with essentially the same value of the average electron density (see Table I). Sample 4 (N_2/H_2 plasma + HMDS) was different, showing a layer of increased electron density extending approximately 1000 Å in depth from the film-air interface. The topmost layer of this sample consists of a region of sharply increased electron density approximately 70 Å thick. The increased electron density may arise from a difference in atomic composition and/or a reduction in porosity in this layer. Interestingly, the bottom layer of this sample has nearly the same electron density as those of the other cured samples. Because our goal in this study was only to characterize the final structure and barrier properties of the cured film, we did not determine whether the nonuniform density profile was due to the N_2/H_2 plasma treatment, the experimental HMDS vapor treatment, or both. However, the reduction in film thickness of sample 4 compared to the uncured sample 1, which was not observed to such an extent in any of the other samples, is suggestive of surface damage during plasma curing.

Certain plasma processes are already known to damage organosilicate low-k materials. For example, Waldfried *et al.* used dynamic secondary-ion mass spectrometry to study the effects of N_2/H_2 plasma and He/H_2 plasma treatments on porous MSQ.[13-15] They found that N_2/H_2 plasma depleted surface carbon, densified the surface, and rendered the films more hydrophilic. The process conditions used in Ref. 13-15 (such as plasma pressure) were different than the curing process used to make sample 4 in this study, but it is possible that the N_2/H_2 plasma curing damaged the surface of sample 4 in a similar fashion. Elsewhere, Lee *et al.* used SXR measurements to illustrate how N_2 plasma treatment of a hydrogensilsesquioxane low-k dielectric can lead to surface densification with a depth of penetration that is dependent upon the processing conditions.[10] Sun *et al.* used positron annihilation spectroscopy to examine how N_2 plasma treatment and O_2 plasma ashing can densify the surface of an MSQ dielectric, reducing film thickness and altering pore structure near the surface.[16] They concluded that N_2 plasma treatment can cause surface densification by collapse of the pores, leaving underlying pores essentially unaffected. Although the materials and processing conditions in Ref. 16 may have been different than those employed here, a pore-collapse mechanism near

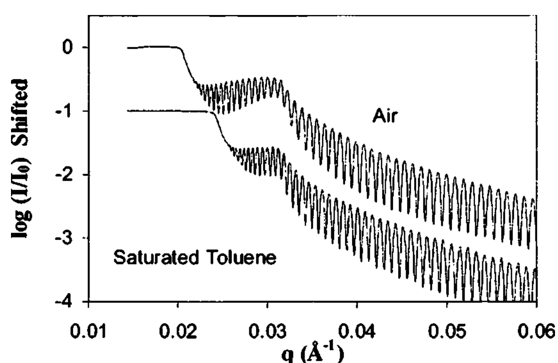

Figure 3. SXR data for sample 3 (N_2/CH_4 plasma cured) in air (top) and saturated toluene vapor (bottom).

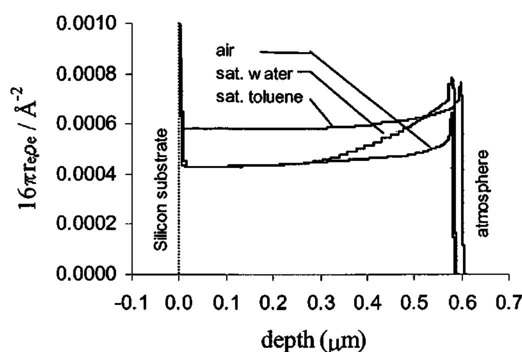

Figure 4. Electron density depth profiles for sample 4 (N_2/H_2 plasma cured + HMDS vapor treated) sample in air, saturated toluene vapor, and saturated water vapor.

the surface is consistent with the loss of thickness and increase in surface density seen in the N_2/H_2 + HMDS sample in this study. The observation that the underlying material has the almost the same density as the other (undamaged) cured samples is also consistent with the observations in Ref. 16. In summary, we postulate that the surface densification in our sample 4 likely occurred during N_2/H_2 plasma curing and may or may not have been enhanced by the HMDS treatment.

The porosity (overall pore volume fraction) of the films was measured using a solvent sorption experiment. When films are exposed to saturated toluene vapor, the pores fill with liquid by capillary condensation. By measuring the electron density of the liquid-filled film, the amount of solvent in the film is deduced (knowing the number of electrons per solvent molecule). Assuming all of the pores fill with solvent, the volume fraction of solvent in the film is equated to the volume fraction of pores. This is probably a reasonable assumption for the MSQ film/toluene system, as toluene is easily able to wet the surface of these films. Toluene is also slightly soluble in the MSQ matrix, suggesting that all pores should be accessible to the solvent, even if they are not directly connected to the surface.

Figure 3 compares SXR data for the N_2/CH_4 plasma-cured sample in air and saturated toluene atmospheres. The critical edge of the film (the first sharp drop in intensity at low q) moves to higher q when the pores are filled with liquid toluene because the overall electron density of the film increases. Based on the toluene uptake, the measured porosity for this sample is (0.41 ± 0.01). From a similar experiment, the measured porosity for sample 1 (uncured) is (0.38 ± 0.01), indicating that much of the porosity is already present after the prebake and softbake steps. Measured porosities of the other cured samples are only slightly different (see Table I). (Standard uncertainties in porosity are estimated at ± 0.01, and similar uncertainties exist in quantities calculated from porosity.) Most of the films exhibited minimal swelling, increasing in thickness by less than 1% when exposed to toluene. However, the N_2/H_2 plasma + HMDS sample increased in thickness by about 3%. The slight swelling of the films in saturated toluene atmosphere supports the assertion that toluene is slightly soluble in the MSQ matrix. The marginal change in film thickness was not expected to affect the calculated porosities substantially.

SXR experiments in saturated water atmosphere were conducted to compare the moisture uptake of the films. Films were exposed to saturated water vapor at 25°C for 3 h followed by measurement of electron density profile by SXR. These measurements did not seek to measure the equilibrium uptake of water, but were a comparison of water uptake after a fixed amount of time. The water uptake (by mass fraction) of the furnace-cured sample was 0.006 ± 0.01, for the N_2/CH_4 plasma-cured sample was 0.026 ± 0.01, and for the $N_2/H_2/CF_4$ plasma-cured sample was 0.040 ± 0.01. The N_2/H_2 plasma + HMDS sample had a higher water uptake of 0.085 ± 0.01. The UV-cured sample had the highest water uptake of any sample, 0.351 ± 0.01. Comparing the results for the different cure processes, it is clear that the curing process significantly alters the barrier properties of the material, likely due to differences in surface chemistry. If the surface is wetted easily by water, the pores are more likely to fill with liquid water in a humid atmosphere.

In this study, the authors did not analyze the changes in film chemistry induced by curing. A previous study[2] employed IR spectroscopy and thermal desorption spectroscopy (TDS) to compare the silanol content between plasma-cured and UV-cured films. The IR measurements were inconclusive because of the weakness of the Si-OH absorption at 950 cm^{-1}. However, TDS measurements recorded a substantially higher evolution of water from the UV-cured film compared to the plasma-cured materials, possibly indicating condensation of silanols. This result supports the idea that the UV-cured material contains substantial Si-OH and therefore is more hydrophilic and conducive to adsorption of atmospheric moisture inside the pores. It is possible that the UV-cured sample contains some unreacted Si-OH from the precursor, or that Si-OH groups could be generated by scission of Si—O—Si linkages if a small amount of atmospheric oxygen were present during the UV cure.

The variability in water uptake may be explained by differences in the silanol (Si-OH) content of the cured films. If the silanol groups are not completely converted to Si—O—Si linkages during curing, then the resulting material may be more hydrophilic.

The water uptake experiment for the N_2/H_2 plasma + HMDS sample indicated a nonuniform uptake of water with respect to film depth after 3 h. Electron density profiles calculated by computer modeling of the SXR data clearly indicated that the water was concentrated within the densified (top) layer of the film, with less water uptake in the remainder of the film (Fig. 4). This result may be due to a gradient in film chemistry or to slow adsorption kinetics hindered by the densified layer on the surface. In contrast to water, toluene was able to permeate the entire film, judging by the electron density profile in saturated toluene atmosphere. This observation supports the idea that toluene is able to wet the surface of this sample throughout the entire film and thus fill all the pores. The wetting is facilitated by the lower surface tension of toluene and by the solubility of toluene in cross-linked MSQ. The experimental HMDS vapor treatment process applied to the N_2/H_2 plasma-cured sample was intended to reduce moisture uptake. However, the SXR results indicate that the HMDS treatment does not completely prevent moisture adsorption in this material. However, elsewhere, HMDS treatment has been successfully employed to increase hydrophobicity in porous organosilicates. For example, Mor *et al.* reported "repair" of porous organosilicate glass damaged by O_2 plasma ashing.[17] They found that HMDS treatment of plasma-damaged films lowers the dielectric constant and reduces leakage current density. These observations were attributed to replacement of silanols with hydrophobic trimethylsilyl groups, which was

thought to discourage moisture uptake. In addition, Clark *et al.* studied HMDS treatment of plasma-damaged MSQ materials, using FTIR spectra to monitor chemical changes.[18] They concluded that isolated hydroxyl groups react with HMDS to form trimethylsilyl groups, whereas hydrogen-bonded silanols are unaffected by exposure to HMDS at 25°C. According to these findings, HMDS treatment does not necessarily remove all hydroxyl content from the material. Thus, in our HMDS-treated sample, it is possible that Si-OH groups are formed during N_2/H_2 plasma curing and that only a fraction of these groups is converted to trimethylsilyl groups during HMDS treatment. This scenario would be consistent with our observation that the N_2/H_2 plasma-cured material retained some hydrophilic character despite HMDS treatment.

Conclusions

SXR measurements can provide detailed information about film structure and barrier properties, facilitating development of low-*k* materials and curing technology. The SXR measurements demonstrated that three of the films (UV, N_2/CH_4 plasma, and $N_2/H_2/CF_4$ plasma) and the furnace-cured film had uniform electron density depth profiles and essentially the same porosity. The N_2/H_2 plasma-cured material that was treated with HMDS was much different, showing a distinct densification at the air-film interface. This film was slightly thinner, had less resistance to swelling in toluene, and showed significant uptake of water, particularly near the film-atmosphere surface when exposed to a humid atmosphere. We postulate that the N_2/H_2 plasma curing damaged the surface of this material, perhaps densifying the film by collapsing pores near the surface, and generated hydrophilic silanol groups, not all of which could be converted to hydrophobic trimethylsilyl groups by treatment with HMDS. Among the other films, which had similar structural features, a wide variation in moisture uptake was noted, with the UV-cured sample exhibiting by far the greatest hydrophilicity. It is possible that hydrophilic silanol groups may have been generated in the UV-cured sample, if a small concentration of atmospheric oxygen was present during curing. Taken together, our results illustrate how curing technology can significantly impact low-*k* barrier properties and therefore affect integration issues.

Acknowledgments

The authors thank Atsushi Shiota and Osamu Aoki from JSR Corporation for providing us with the materials for this study. The National Institute of Standards and Technology Office for Microelectronics Programs is gratefully acknowledged for support.

The National Institute of Standards and Technology assisted in meeting the publication costs of this article.

References

1. U.S. patents pending.
2. C. Waldfried, A. Shiota, O. Escorcia, Q. Han, and I. Berry, in *Copper Interconnects, New Contact Metallurgies, and Low-k Interlevel Dielectrics*, G. S. Mathad, H. S. Rathore, C. Reidsema-Simpson, T. L. Ritzdorf, and B. Baker, Editors, PV 2002-22, p. 187, The Electrochemical Society Proceedings Series, Pennington, NJ (2003).
3. C. Waldfried, Q. Han, O. Escorcia, A. Margolis, R. Albano, and I. Berry, in *IEEE International Interconnect Technology Conference Proceedings*, San Francisco, CA, IEEE, p. 226 (2002).
4. C. Waldfried, Q. Han, O. Escorcia, R. Albano, and I. Berry, in *Proceedings of the Sematech Ultra-Low-k Workshop*, International Sematech, San Francisco, CA (2002).
5. C. Waldfried, A. Margolis, Q. Han, O. Escorcia, R. Albano, and I. Berry, in *Rapid Thermal and Other Short-Time Processing Technologies III*, P. Timans, E. Gusev, F. Roozeboom, M. Oztürk, and D. L. Kwong, Editors, PV 2002-11, p. 53, The Electrochemical Society Proceedings Series, Pennington, NJ (2002).
6. Q. Han, W. Chen, C. Waldfried, O. Escorcia, T. J. Bridgewater, E. S. Moyer, and I. Berry, in *Proceedings of the 1st International Conference on Semiconductor Technology (ISTC) 2001*, Vol. 2, p. 234 (2001).
7. A. Shiota, M. Sekiguchi, H. Nakagawa, M. Mita, and T. Yamanaka, in *Proceedings of the Sematech Ultra-Low-k Workshop*, International Sematech, San Francisco, CA (2002).
8. E. K. Lin, H.-J. Lee, G. W. Lynn, W.-L. Wu, and M. L. O'Neill, *Appl. Phys. Lett.,* **81**, 607 (2002).
9. H.-J. Lee, E. K. Lin, H. Wang, W.-L. Wu, W. Chen, and E. S. Moyer, *Chem. Mater.,* **14**, 1845 (2002).
10. H.-J. Lee, E. K. Lin, W.-L. Wu, B. M. Fanconi, J. K. Lan, Y. L. Cheng, H. C. Liou, Y. L. Wang, M. S. Feng, and C. G. Chao, *J. Electrochem. Soc.,* **148**, F195 (2001).
11. B. J. Bauer, E. K. Lin, H. J. Lee, H. Wang, and W.-L. Wu, *J. Electron. Mater.,* **30**, 304 (2001).
12. W.-L. Wu, W. E. Wallace, E. K. Lin, G. W. Lynn, C. J. Glinka, E. T. Ryan, and H. M. Ho, *J. Appl. Phys.,* **87**, 1193 (2000).
13. C. Waldfried, Q. Han, O. Escorcia, I. Berry, and E. Andideh, in *2003 VMIC Proceedings*, p. 180 (2003).
14. C. Waldfried, Q. Han, O. Escorcia, and P. B. Smith, *Electrochem. Solid-State Lett.,* **6**, G137 (2003).
15. C. Waldfried, Q. Han, O. Escorcia, and I. Berry, in *Proceedings of the First International Surface Cleaning Workshop*, Northeastern University, Boston, MA (2002).
16. J. N. Sun, D. W. Gidley, Y. Hu, W. E. Frieze, and E. T. Ryan, *Appl. Phys. Lett.,* **81**, 1447 (2002).
17. Y. S. Mor, T. C. Chang, P. T. Liu, T. M. Tsai, C. W. Chen, S. T. Yan, C. J. Chu, W. F. Wu, F. M. Pan, W. Lur, and S. M. Sze, *J. Vac. Sci. Technol. B,* **20**, 1334 (2002).
18. P. G. Clark, B. D. Schwab, J. W. Butterbaugh, H. J. Martinez, and P. J. Wolf, *Semicond. Int.,* **26**, 46 (2003).